Front. Struct. Civ. Eng. 2017, 11(1): 111–122
DOI 10.1007/s11709-016-0354-x

RESEARCH ARTICLE

Predication of discharge coefficient of cylindrical weir-gate using adaptive neuro fuzzy inference systems (ANFIS)

Abbas PARSAIE[a,*], Amir Hamzeh HAGHIABI[a], Mojtaba SANEIE[b], Hasan TORABI[a]

[a] *Department of Water Engineering, Lorestan University, Khorramabad, Iran*

[b] *Soil Conservation and Watershed Management Research Institute, Tehran, Iran*

[*] *Corresponding author. E-mail: Abbas_Parsaie@yahoo.com*

ABSTRACT Settlement of sediments behind weirs and accumulation of materials floating on water behind gates decreases the performance of these structures. Weir-gate is a combination of weir and gate structures which solves them Infirmities. Proposing a circular shape for crest of weirs to improve their performance, investigators have proposed cylindrical shape to improve the performance of weir-gate structure and call it cylindrical weir-gate. In this research, discharge coefficient of weir-gate was predicated using adaptive neuro fuzzy inference systems (ANFIS). To compare the performance of ANFIS with other types of soft computing techniques, multilayer perceptron neural network (MLP) was prepared as well. Results of MLP and ANFIS showed that both models have high ability for modeling and predicting discharge coefficient; however, ANFIS is a bit more accurate. The sensitivity analysis of MLP and ANFIS showed that Froude number of flow at upstream of weir and ratio of gate opening height to the diameter of weir are the most effective parameters on discharge coefficient.

KEYWORDS weir-gate, soft computing, crest geometry, circular crest weir, cylindrical shape

1 Introduction

Modeling the hydraulic structure in real conditions is the main part of hydraulic engineering studies. Weirs and gates are the most common structures, which have been widely used in water resource projects such as irrigation and drainage networks [1,2]. As definition states, any obstacle standing on the way of water flow is called a weir. Construction of weirs on waterways reduces the velocity of flow at the upstream weirs that leads to settlement of suspended sediment [3–14]. Defining the hydraulic properties of flow over weirs is usually conducted under clean water conditions. In other words, in most studies, the effect of suspended sediment loads has been ignored, whereas in real hydraulic projects water flows always include some suspended loads [12,13,15–19]. Settlement of sediments in upstream of weirs has lead to the change of defined hydraulic properties, which are derived in laboratory experiment conditions or theoretical formulas, which have been proposed to this purpose. Israelsen and Hansen [20] stated that when depth of tapped sediments is close to 75 percent of weir height, discharge is calculated eight percent more than the real data. Gates are other structures which are widely used in water engineering projects as well. The main points related to gates are accumulation of suspended material behind them. This condition caused to change the condition of derived governing equation to real situations. Improving the performance of hydraulic structures is a major part of hydraulic engineering activities. One way to solve the infirmity of both mentioned structures is proposing a new structure, which is a combination of both weir and gate called weir-gate structure. Negm et al. [21] have studied hydraulic properties of V-Notches weir-gate. They proposed an equation to calculate diacharge coefficient of weir-gate steucture. Negm et al. [22] studied the effects of hydraulic and geometric parameters on discharge coefficient of rectangular weir-gate structure and realized that using conventional weir discharge coefficient leads to unacceptable errors for discharge calculation. Using Π theorem as a dimensional analysis technique, Ferro [23] derived parameters involved in discharge coefficient of weir-gate

Article history: Received Feb 6, 2016; Accepted Apr 10, 2016

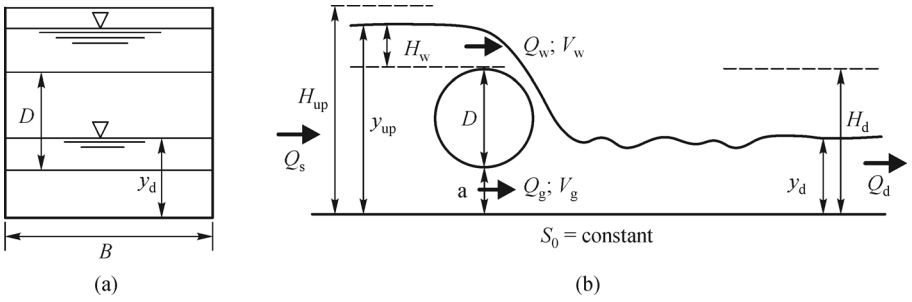

Fig. 1 Sketch of cylindrical weir-gate and its hydraulic parameters

structure. He stated that the ratio of critical depth relative to specific discharge to the opening height of the gate and the ratio of total upstream head to the opening height of the gate are the most effective parameters on discharge coefficient. Negm et al. [24] proposed an equation for rectangular weir-gate with lateral contraction. They stated that the ratio of total upstream head to the opening height and the ratio of flow depth on opening height of the gate are affective parameters for modeling discharge coefficient of weir-gate structure. By advancing of experimental studies on weir hydraulics, investigators have evaluated various forms for crest of weirs. Among various forms of weir's crest, the cylindrical form has been welcomed by the researchers due to its high capacity for passing the flow [25]. References [26,27] have conducted extensive studies on flow characteristics over circular crest weir. They stated that the ratio of total upstream head to the ratio of crest is the most effective parameter on discharge coefficient of circular crest weir [28–30]. Using circular crest concept, investigators have tried to develop and improve the performance of weir-gate by proposing cylindrical weir-gate [31]. Figure 1 shows a schematic shape of cylindrical weir-gate and its geometric and hydraulic parameters. Cylindrical weir-gate as shown in the Fig. 1 can smoothly pass the flow over and under the structure. Investigators have studied the hydraulic properties of weir-gate structure using laboratory experiments.

In Fig. 1, Q_s is discharge in main channel, y_{up}= upstream flow depth, H_{up} = total head of flow at upstream, Q_w = weir discharge, Q_g gate discharge, H_w depth of flow on the crest, Q_d = downstream discharge, y_d = downstream discharge, a = gate opening height, V_g = velocity of flow under the gate, V_w = overflow velocity, V_a = mean velocity, S_0 = bed slope of main channel, D = diameters of cylinder. Recently, by advancement in soft computing techniques in water resource management for accurately modeling hydraulic phenomena [7–9,32–41], researchers have attempted to use these techniques for modeling discharge coefficient of hydraulic structures especially for weirs. Juma et al. [42] used neural network techniques for modeling discharge coefficient of circular crest weir. They stated that the neural network has a high ability for modeling discharge coefficient of circular crest weir. Up to now, authors have not found any report on modeling discharge coefficient of cylindrical weir-gate using illustrated soft computing techniques in the materials and methods section. Therefore, in this study, the performance of two soft computing techniques (ANFIS and MLP) was evaluated for modeling and predicting discharge coefficient of cylindrical weir-gate.

2 Materials and methods

As shown in the literature, several hydraulic and geometric parameters are involved in discharge coefficient of cylindrical weir-gate. In Eq. (1), the involved factors have come together.

$$f(Q_s,y_{up},y_d,H_w,a,V_w,V_g,D,\delta,B,S_0,g,\mu,\rho,\sigma,C_{ds}) = 0, \quad (1)$$

where B = width of main channel, g = gravity acceleration, σ = surface tension, δ = amount of contraction, μ = kinematic viscosity, ρ = fluid density, C_{ds} = discharge coefficient of weir-gate. Assessing the component of involved parameters shows that three basic components including length (L), time (T) and mass (M) are presented; therefore, using Π theorem as dimensional analysis and with regarding Eq. (1) and basic components, 13(16–3 = 13) dimensionless parameters are derived, as presented in Eq. (2). It is notable that during derivation of dimensionless parameters, three variables including D (L), $g(m/t^2)$ and $\rho(m/l^3)$ were considered as repetitive parameters.

$$g\left(\frac{Q_s}{g^{0.5}y_{up}^{2.5}},\frac{y_{up}}{D},\frac{y_d}{D},\frac{H_w}{D},\frac{a}{D},Fr_w,Fr_g,\frac{\delta}{D},\frac{B}{D},S_0,\right.$$

$$\left.\mathrm{Re}_{up},We_{up},Cd_{ds}\right) = 0. \quad (2)$$

Investigators have always attempted to keep turbulent flow condition in their studies; therefore, the effect of

viscosity (Re_{up}) is removed and have adherence to the minimum depth as well, so that the Weber number (We_{up}) can be ignored. Based on the published reports, in experiments, usually the width of main channel and longitudinal channel slope remain constant; therefore, δ/D, B/D and S_0 have constant values. Instead of measuring the Froude number of flow over and below the structure (Fr_w,Fr_g), the upstream Froude number (Fr_{up}) has been measured. Equation (2) can be rewritten as Eq. (3).

$$f\left(\frac{Q_s}{g^{0.5}y_{up}^{2.5}},\frac{y_{up}}{D},\frac{y_d}{D},\frac{H_w}{D},\frac{a}{D},Fr_{up},Cd_{ds}\right)=0. \quad (3)$$

With combination of both dimensionless parameters (y_{up}/D and y_d/D) as below, the new form of Eq. (3) is derived as Eq. (4). It is notable that the term $Q_s/g^{0.5}y_{up}^{2.5}$ is familiar to the Froude number; therefore, the upstream Froude number is a suitable proxy to show the effect of this parameter. The flow was presorted subcritical in experiments. Therefore, control of flow is conducted at the upstream and the effect of tail water (y_d) is negligible.

$$\frac{y_{up}/D}{y_d/D}=\frac{y_{up}}{y_d},$$

$$Cd_{ds}=\left(Fr_{up},\frac{H_w}{D},\frac{a}{D}\right). \quad (4)$$

In Table 1, 89 data sets related to involved parameters on discharge coefficient of weir-gate are collected from Severi et al. [31]. These data are used for developing ANFIS and MLP models.

3 Artificial neural networks (ANNs)

ANN is a nonlinear mathematical model that is able to simulate many complex mathematical system that relate inputs and outputs. Multilayer perceptron (MLP) networks are common types of ANN widely used in the research. To use MLP model, definition of appropriate functions, weights and bias should be considered. Due to the nature of the problem, different activity functions in neurons can be used. An ANN may have one or more hidden layers. Figure 1 demonstrates a three-layer neural network consisting of inputs layer, hidden layer (layers) and outputs layer. As shown in Fig. 4, w_i is the weight and θ_i is the bias for each neuron. Weight and biases' values will be assigned progressively and corrected during training process comparing the predicted outputs with known ones. Such networks are often trained using back propagation algorithm. In the present study, MLP was trained by Levenberg–Marquardt technique, since this technique is more powerful and faster than the conventional gradient descent technique [7–9].

4 Adaptive neuro fuzzy inference systems (ANFIS)

Adaptive neuro fuzzy inference system (ANFIS) is a powerful tool for modeling complex systems based on input and output data. ANFIS is realized by an appropriate combination of neural and fuzzy systems. This combination enables using both numeric powers of intelligent systems. In fuzzy systems, different fuzzification and defuzzification strategies with different rules were considered for inputs parameter. For carried out the effect of fuzzy logic on inputs data, three stages should be considered. Stage one is selecting membership function for each inputs variable. In this stage, a Gaussian function may be considered for each of inputs variables. Figure 3 shows a fuzzy reasoning process. For simplicity, a fuzzy system with two inputs and one output variable was considered. Suppose that the rule base contains two fuzzy if-then rules.

$$\text{Rule 1}: \text{ if } x \text{ is } A_1 \text{ and } y \text{ is } B_1, \text{then } f_1 = p_1x + q_1y + r_1,$$

$$\text{Rule 1}: \text{ if } x \text{ is } A_2 \text{ and } y \text{ is } B_2, \text{then } f_2 = p_2x + q_2y + r_2,$$

where A_1, A_2 and B_1, B_2 are MFs for inputs x and y, respectively; p_1, q_1, r_1 and p_2, q_2, and r_2 are parameters of output function. ANFIS architecture is presented in Fig. 3 (b). In the first layer, all inputs variables gave the grade membership with membership function and in layer 2, all membership grades will be multiplied together. In layer 3, all grades of member will be normalized and in layer 4, the contribution of all rules will be computed. And in the last layer, output variable will be computed as weighted average of grade membership [16].

5 Results and discussion

5.1 Results of ANNs

Preparation of multilayer perceptron (MLP) neural network model as a common type of ANN models through soft-computing techniques is based on the data set. Therefore, collected data set was divided into three groups as training, validation and testing data set. Validation data set was considered for avoiding overtraining of ANN model. The dimensionless parameters, presented in Eq. (4), were desirable as input parameters for MLP model development and discharge coefficient was considered as model output. Data selection for preparation of MLP model was carried out using randomly approach. Seventy percent of total data set was considered for training, 15 percent for validation and the rest (15 percent) for testing.

Table 1 Summary of collected data [31]

row	a/D	H_W/D	Fr_{up}	C_{ds}	row	a/D	H_W/D	Fr_{up}	Cd_{ds}
1	0.00	0.62	0.28	1.37	46	0.27	0.62	0.26	0.85
2	0.00	0.52	0.30	1.37	47	0.27	0.55	0.27	0.89
3	0.00	0.44	0.32	1.38	48	0.27	0.35	0.29	0.93
4	0.00	0.33	0.34	1.38	49	0.27	0.27	0.31	0.97
5	0.00	0.11	0.35	1.40	50	0.40	1.13	0.27	0.73
6	0.00	0.99	0.37	1.40	51	0.40	1.04	0.28	0.76
7	0.20	1.37	0.30	1.04	52	0.40	0.95	0.30	0.80
8	0.20	1.28	0.32	1.08	53	0.40	0.85	0.31	0.83
9	0.20	1.18	0.33	1.11	54	0.53	0.41	0.31	0.70
10	0.20	1.08	0.36	1.12	55	0.53	0.31	0.33	0.73
11	0.20	0.97	0.37	1.17	56	0.00	1.08	0.14	1.25
12	0.20	0.85	0.39	1.19	57	0.00	1.02	0.15	1.28
13	0.40	1.13	0.31	0.80	58	0.00	0.97	0.16	1.28
14	0.40	1.04	0.32	0.85	59	0.00	0.9	0.18	1.30
15	0.40	0.95	0.34	0.89	60	0.00	0.83	0.19	1.32
16	0.40	0.85	0.36	0.94	61	0.00	0.75	0.21	1.35
17	0.40	0.73	0.38	0.97	62	0.09	0.59	0.15	0.94
18	0.40	0.61	0.39	1.01	63	0.09	0.54	0.16	0.97
19	0.60	0.92	0.32	0.66	64	0.09	0.5	0.17	1.01
20	0.60	0.83	0.33	0.71	65	0.09	0.38	0.19	1.04
21	0.60	0.73	0.35	0.75	66	0.09	0.32	0.20	1.09
22	0.60	0.62	0.36	0.79	67	0.09	0.28	0.21	1.13
23	0.60	0.5	0.38	0.83	68	0.18	0.5	0.17	0.77
24	0.60	0.33	0.39	0.87	69	0.18	0.44	0.18	0.81
25	0.80	0.55	0.36	0.64	70	0.18	0.39	0.19	0.83
26	0.80	0.5	0.37	0.66	71	0.18	0.33	0.20	0.86
27	0.80	0.47	0.37	0.69	72	0.18	0.26	0.21	0.89
28	0.80	0.73	0.39	0.71	73	0.18	0.16	0.22	0.93
29	0.80	0.37	0.40	0.74	74	0.00	1.55	0.12	1.22
30	1.00	0.5	0.40	0.62	75	0.00	1.26	0.13	1.24
31	1.00	0.36	0.40	0.64	76	0.00	1.22	0.15	1.25
32	0.00	0.76	0.20	1.32	77	0.00	1.21	0.16	1.27
33	0.00	0.72	0.22	1.34	78	0.00	1.18	0.17	1.30
34	0.00	0.68	0.23	1.35	79	0.00	1.16	0.18	1.32
35	0.00	0.64	0.25	1.37	80	0.08	0.5	0.13	0.94
36	0.00	0.59	0.27	1.40	81	0.08	0.47	0.15	0.95
37	0.00	0.54	0.28	1.40	82	0.08	0.43	0.17	1.01
38	0.13	0.91	0.21	0.98	83	0.08	0.37	0.18	1.05
39	0.13	0.85	0.23	1.02	84	0.08	0.32	0.18	1.08
40	0.13	0.8	0.25	1.06	85	0.08	0.26	0.20	1.10
41	0.13	0.72	0.26	1.08	86	0.16	0.42	0.16	0.81
42	0.13	0.65	0.28	1.13	87	0.16	0.37	0.18	0.83
43	0.13	0.57	0.30	1.16	88	0.16	0.3	0.19	0.90
44	0.27	0.74	0.23	0.78	89	0.16	0.27	0.20	0.92
45	0.27	0.68	0.24	0.82					

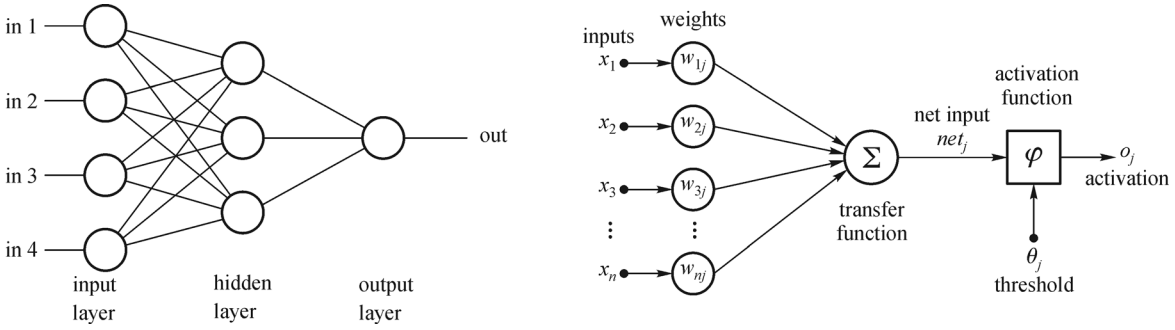

Fig. 2 Sketch of three-layer ANN architecture

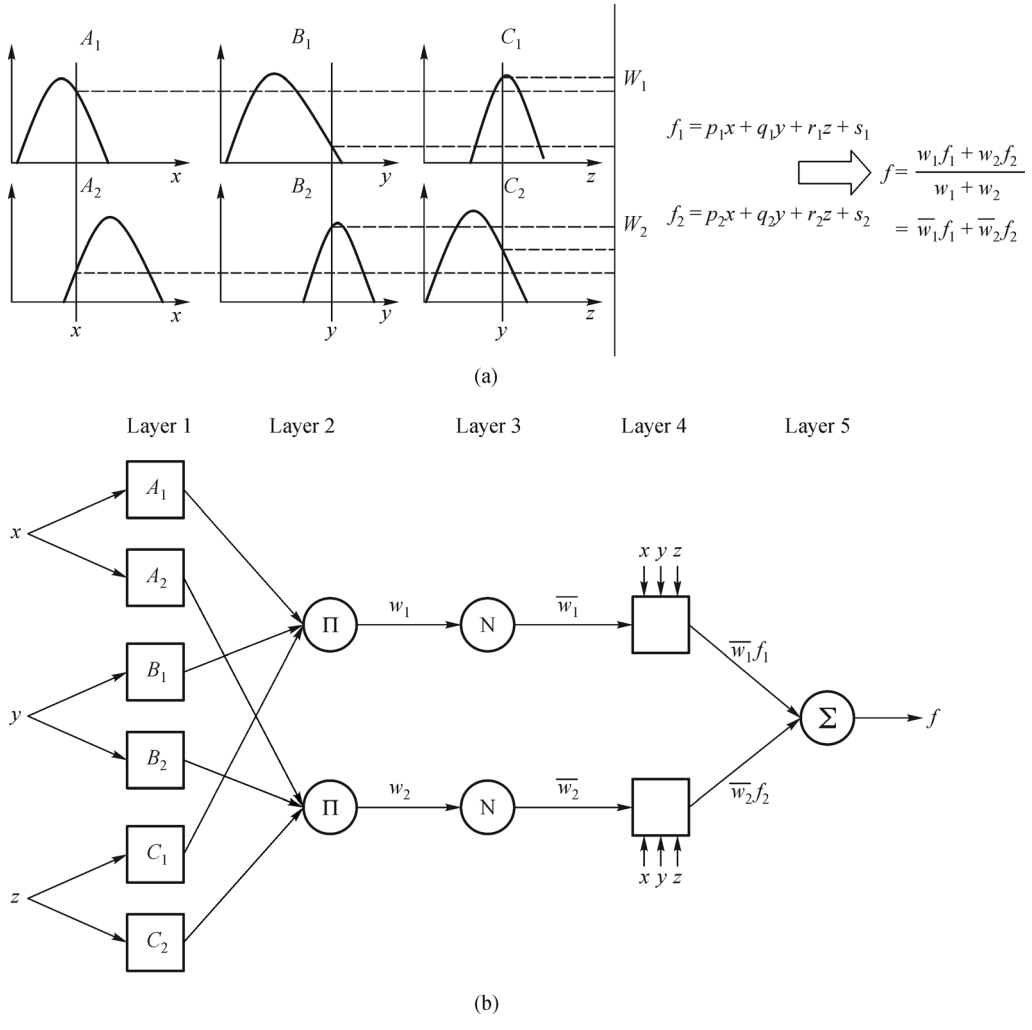

Fig. 3 ANFIS model structure

Designing the architect of MLP model is mostly based on designer's experience, whereas recommendation of investigators, who conducted similar research, is useful. In this paper, recommendations of Parsaie and Haghiabi [7–9] were used. Preparation of MLP model includes the number of hidden layer(s), number of neurons in each hidden layer, defining suitable transfer function for neurons of hidden layer(s), defining suitable transfer function for output layer and learning algorithm. To obtain an optimal structure and avoid the over- parameterization of MLP model, first, one

Table 2 Performance and summary of MLP model during development stage

row	N-H-L	F-HL&TF	S-HL&TF	during training stage			during testing stage		
				R^{2*}	MSE*	RMSE *	R^{2*}	MSE*	RMSE*
1	1	5-Purelin	-	0.91	0.0007	0.0073	0.83	0.004	0.09
2	1	13-Purelin	-	0.94	0.0003	0.0055	0.96	0.003	0.06
3	1	5-tansig	-	0.998	0.000081	0.009	0.991	0.0004	0.021
4	4	9-tansig	-	0.998	0.000061	0.007	0.993	0.0003	0.017

Note: N-H-L: number of hidden layer(s), F-HL&TF: first hidden layer and transfer function, S-HL&TF: second hidden layer and transfer function,*error indices of MLP

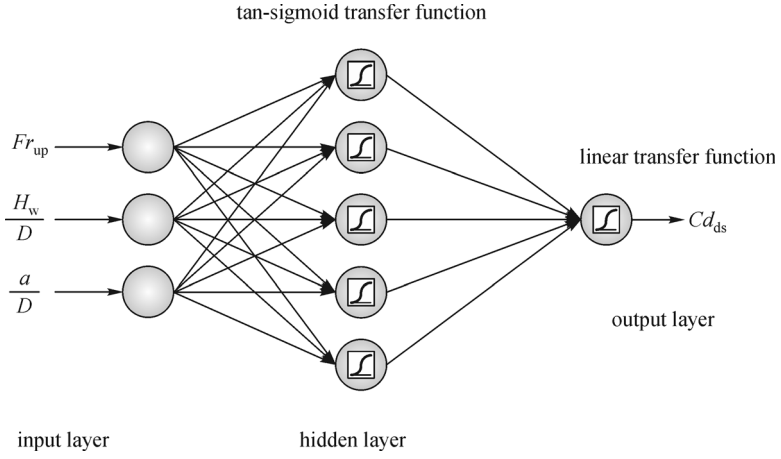

Fig. 4 Architect of developed ANN

hidden layer was considered and then, the number of neurons in hidden layer is increased one by one. Various types of transfer functions such as log-sigmoid (logsig), tan-sigmoid (tansig), and linear (purelin) etc. were tested. This process continues to obtain a model with suitable performance. All stages of MLP preparation were conducted in the environment of MATLAB software. Table 2 presents a summary of trial and error process conducted during MLP model.

As presented in Table 2, model number 3 has suitable performance for predicting discharge coefficient and increasing the number of neurons in hidden layer does not have a significant effect on increasing model performance. As presented in Table 2, MLP model number 3 has one hidden layer with five neurons. The tansig and purelin functions were considered as transfer function for hidden and output layers transfer function respectively. The developed MLP model structure is shown in Fig. 4. The mean square error of MLP during training is shown in Fig. 9. It is notable that the Levenberg–Marquardt technique was used for MLP model learning.

Results of MLP model during training, validation and testing stages are shown in Figs. 5, 6 and 7. In these figures, results of MLP model were plotted together with measured data. To evaluate model precision, the standard error indices were also calculated and presented in these figures. Since error indices present an average value for error calculation, distribution of error for the training, validation and testing data sets was also plotted. To give more information about error distribution, the histogram of errors was also plotted. As seen from these figures, the error distribution is focused around zero for training, validation and testing.

5.2 Sensitivity analysis of effective parameters

The most effective parameters for prediction of discharge coefficient by ANN were defined via simple approach. This approach describes the effect of each parameter on model performance to predict the output [43–46]. First, regarding to Eq. (2), all parameters are considered as inputs for ANN. Then, one of the input parameters is removed from input parameters and again the model is prepared with the same structure. It is notable that preparation of models was considered regarding the notes in model development section. Performance of models in absence of each input parameter is assessed using calculation of error indices including $R^2$and RMSE. Obviously, removing one of input parameters causes the change of model performance. Depending on the severity of performance changing, the effect of each parameter is assessed. Results of sensitivity analysis of MLP are given in Table 3. As seen

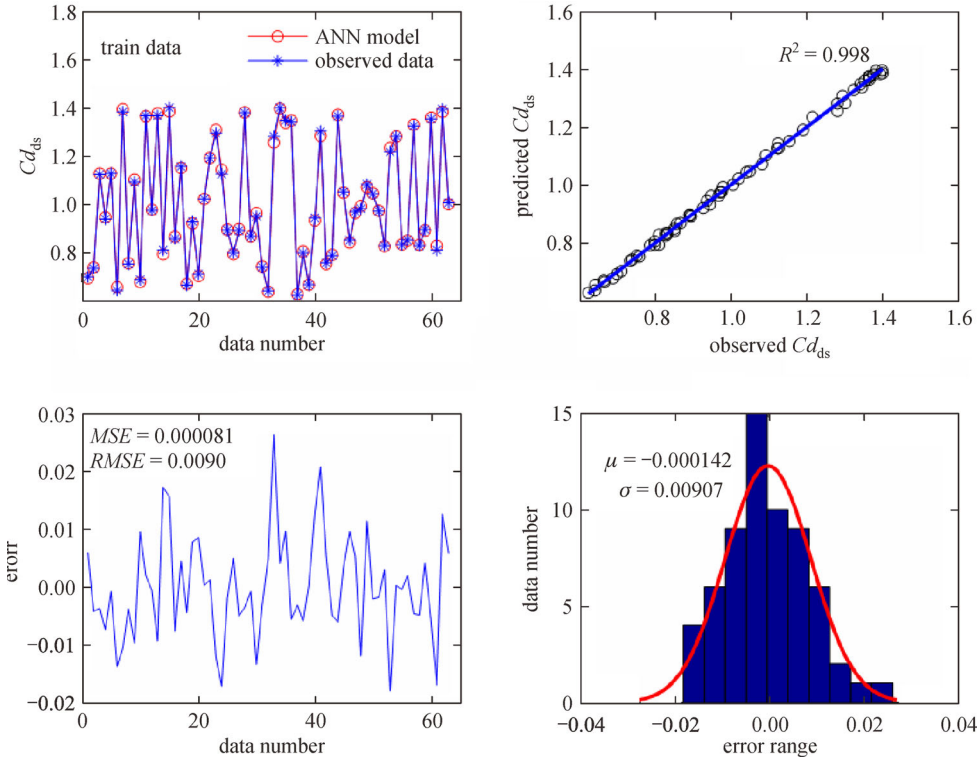

Fig. 5 Performance of ANN in training stage

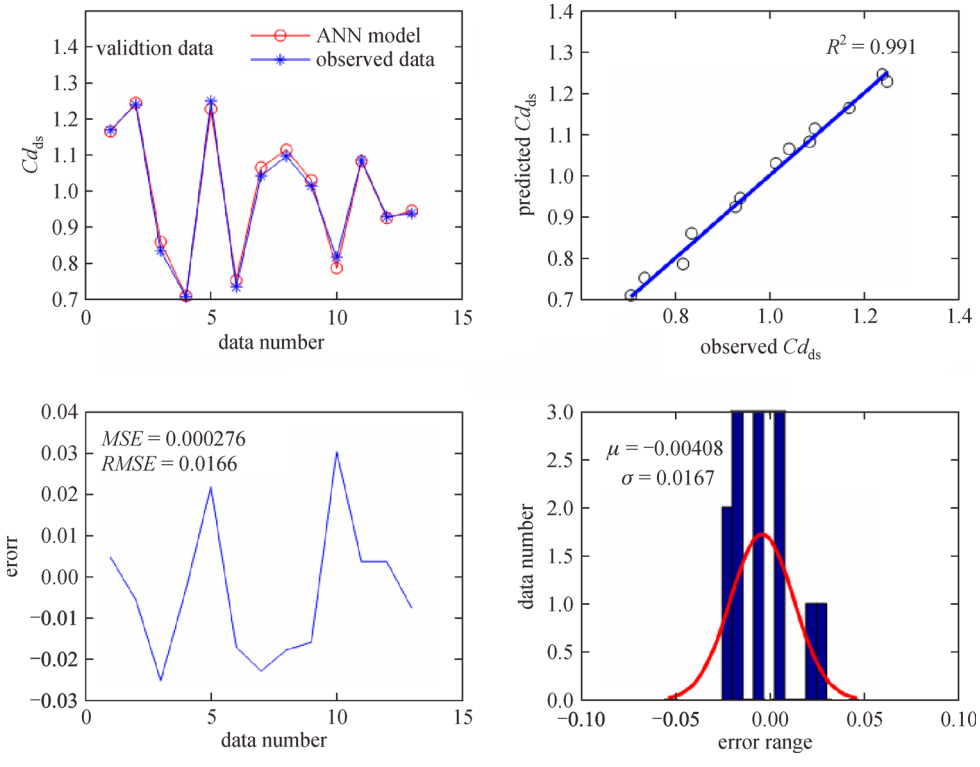

Fig. 6 Performance of ANN in validation stage

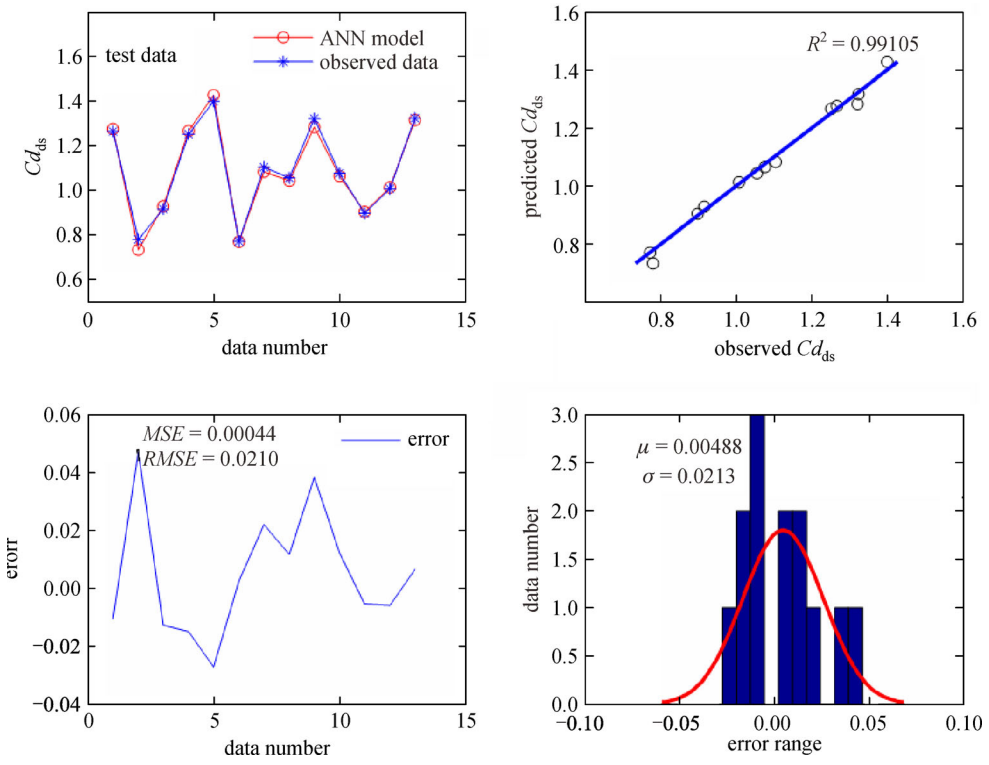

Fig. 7 Performance of ANN in testing stage

in Table 3, absence of Froude number (Fr_{up}) and a/D causes a dramatic decrease in the accuracy of models; therefore, it was found that these parameters are the most important ones for modeling discharge coefficient of side weir.

5.3 Results of ANFIS

Similar to artificial neural network models (MLP) preparation, developing ANFIS model is based on data set. Compared to other ANN models such as Multilayer perceptron neural network (MLP) model, the main advantage of ANFIS is its utility in stage of designing the structure of model and this utility is related to specifying the number of membership function to inputs variable based on its influence on output parameter. This utility of ANFIS model leads to developing a model that is more optimal and has more reliability, since each parameter, which is more effective on outputs, can get more membership function. In this study, results of MLP are used to develop an optimal structure. Data sets are randomly divided into two groups as training and testing. Based on the results of MLP, 71 data sets (80 percent) of collected data were considered for ANFIS model training and the rest (20 percent = 18) for model testing. The structure of ANFIS, which has the best performance, is given in Table 4. As shown in Table 4, the Gaussian function (guassmf) was considered for membership function and weight average (wtaver) approach was considered for defuzzification method. Figure 8 is the performance of ANFIS model during training stage and Fig. 9 shows the results of ANFIS model for testing data. As shown in Figs. 8 and 9, the histogram and distribution of errors are also plotted to assess the performance of ANFIS model in training and testing stages. In overall, as shown in Figs. 8 and 9 the ANFIS model's ability is suitable for predicting the values of discharge coefficient in training and testing stages. As seen from Table 4, the most affective input variables such as Fr_{up} and a/D get more memebrship fucntion compared to other variables during ANFIS model development. The histogram of error shows that values of error focus around zero and histoagram is almost symmetric.

Table 3 Results of sensitivity analysis of ANN

model	absent	inputs	output	R^2	RMSE
MLP	-	Fr_{up}, H_w/D, a/D	Cd_{sd}	0.99	0.021
	Fr_{up}	H_w/D, a/D	Cd_{sd}	0.78	0.075
	H_w/L	Fr_{up}, a/D	Cd_{sd}	0.91	0.038
	a/D	Fr_{up}, H_w/D	Cd_{sd}	0.86	0.143

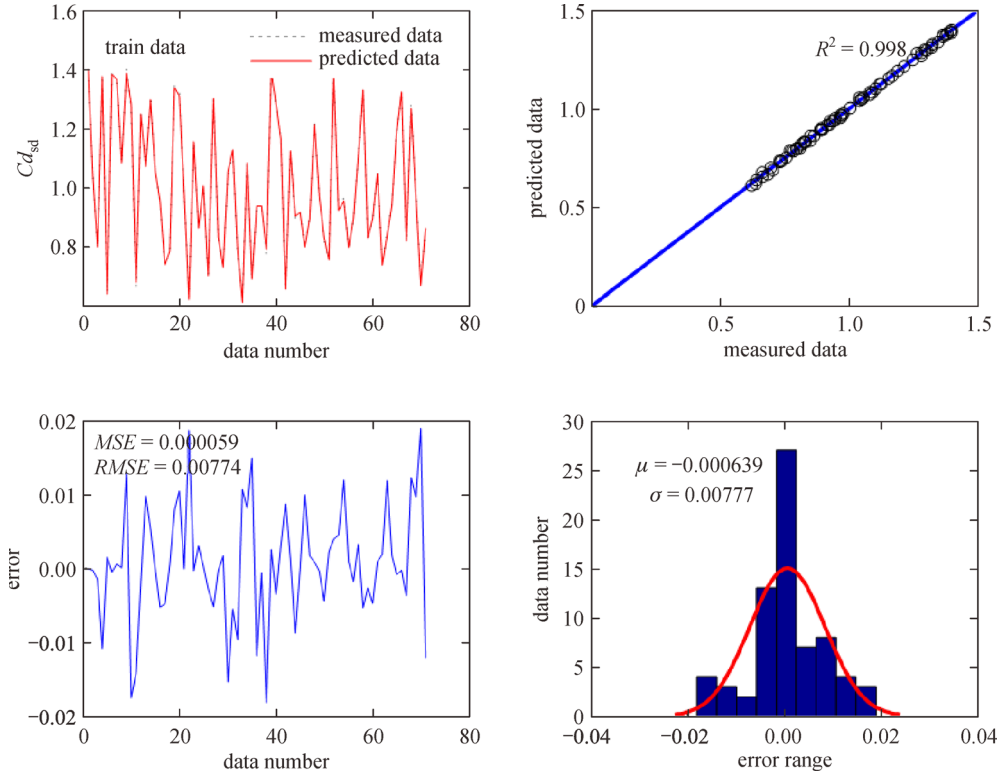

Fig. 8 Performance of ANFIS model during training stage

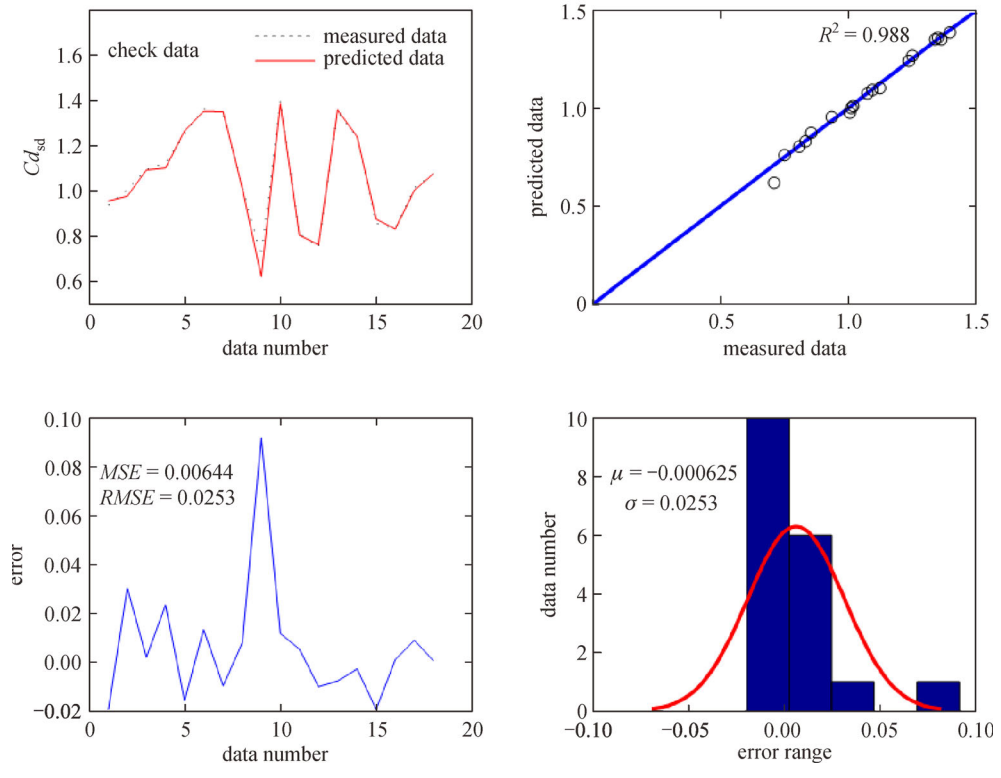

Fig. 9 Performance of ANFIS model during testing stage

Table 4 Performances and Summery of the ANFIS Structure

parameter	Nmf	MF	and method	or method	defuzz method	agg method	type	R^2		RMSE	
								train	test	train	test
Fr_{up}	6	gaussmf	prod	max	wtaver	max	sugeno	0.99	0.99	0.030	0.045
H_w/D	3	gaussmf	prod	max	wtaver	max					
a/D	4	gaussmf	prod	max	wtaver	max					

Note: Nmf: number of membership functions, MF: membership function

Table 5 Results of ANFIS sensitivity analysis

Absent	inputs	output	R^2	RMSE
-	Fr_{up}, H_w/D, a/D	Cd_{sd}	0.99	0.025
Fr_{up}	H_w/D, a/D	Cd_{sd}	0.71	0.094
H_w/D	Fr_{up}, a/D	Cd_{sd}	0.93	0.032
a/D	Fr_{up}, H_w/D	Cd_{sd}	0.91	0.041

5.4 Sensitivity analysis of ANFIS

To assess performance of developed ANFIS model in absence of each input, a sensitivity analysis was carried out on ANFIS model. This process has another advantage related to the response of developed optimal ANFIS model in absence of input parameters. Regarding this approach, which was considered for sensitivity analysis of ANN, sensitivity analysis of ANFIS also was conducted. Results of sensitivity analysis of ANFIS are given in Table 5. Overviewing Table 5 uphold the results of sensitivity analysis of ANN whereas Table 5 shows that the structure of developed ANFIS is more sensitive to the absence of important parameters and has less sensitivity to the absence of each parameters which are less important.

6 Conclusion

Weir-gate is a structure which solves the infirmity of weir and gate separately in real conditions of usage in water engineering projects. Recently, implementing soft-computing techniques for modeling systems, which are based on input and output data set investigators have attempted to use these methods to increase precision of modeling. In this study, discharge coefficient of weir-gate was predicted using adaptive neuro fuzzy inference systems (ANFIS) and multilayer perceptron neural network (MLP). Results of MLP indicated that the Froude number of flow at upstream of weir and ratio of gate opening height to diameter of weir are the most effective parameters on discharge coefficient. Results of MLP and ANFIS showed that these models have so suitable performance for modeling and predicting discharge coefficient of weir-gate.

References

1. Dehdar-behbahani S, Parsaie A. Numerical modeling of flow pattern in dam spillway's guide wall. Case study: Balaroud dam, Iran. Alexandria Engineering Journal, 2016, 55(1): 467–473
2. Parsaie A, Haghiabi A H, Moradinejad A. CFD modeling of flow pattern in spillway's approach channel. Sustainable Water Resources Management, 2015, 1(3): 245–251
3. Budarapu P R, Gracie R, Yang S W, Zhuang X, Rabczuk T. Efficient coarse graining in multiscale modeling of fracture. Theoretical and Applied Fracture Mechanics, 2014, 69: 126–143
4. Budarapu P R, Yb S S, Javvaji B, Mahapatra D R. Vibration analysis of multi-walled carbon nanotubes embedded in elastic medium. Frontiers of Structural and Civil Engineering, 2014, 8(2): 151–159
5. Budarapu P R, Javvaji B, Sutrakar V K, Roy Mahapatra D, Zi G, Rabczuk T. Crack propagation in graphene. Journal of Applied Physics, 2015, 118(6): 064307
6. Budarapu P R, Narayana T S S, Rammohan B, Rabczuk T. Directionality of sound radiation from rectangular panels. Applied Acoustics, 2015, 89: 128–140
7. Parsaie A, Haghiabi A. The effect of predicting discharge coefficient by neural network on increasing the numerical modeling accuracy of flow over side weir. Water Resources Management, 2015, 29(4): 973–985
8. Parsaie A, Haghiabi A H.Computational modeling of pollution transmission in rivers. Applied Water Science, 2015, 89: 1–10
9. Parsaie A, Haghiabi A H. Predicting the longitudinal dispersion coefficient by radial basis function neural network. Modeling Earth Systems and Environment, 2015, 1(4): 1–8
10. Sudhir Sastry Y B, Budarapu P R, Krishna Y, Devaraj S. Studies on ballistic impact of the composite panels. Theoretical and Applied Fracture Mechanics, 2014, 72: 2–12
11. SudhirSastry Y B, Budarapu P R, Madhavi N, Krishna Y. Buckling analysis of thin wall stiffened composite panels." Computational Materials Science, 2015, 96(B): 459–471

12. Talebi H, Silani M, Bordas S P A, Kerfriden P, Rabczuk T. A computational library for multiscale modeling of material failure. Computational Mechanics, 2013, 53(5): 1047–1071
13. Talebi H, Silani M, Bordas S P A, Kerfriden P, Rabczuk T. Molecular dynamics/XFEM coupling by a three-dimensional extended bridging domain with applications to dynamic brittle fractures. 2013, 11(6): 527–541
14. Yang S W, Budarapu, P R, Mahapatra, D R, Bordas S P A, Zi G, Rabczuk T. A meshless adaptive multiscale method for fracture. Computational Materials Science, 2015, (B): 382–395
15. Amiri F, Millán D, Shen Y, Rabczuk T, Arroyo M. Phase-field modeling of fracture in linear thin shells. Theoretical and Applied Fracture Mechanics, 2014, 69: 102–109
16. Azamathulla H M, Haghiabi A H, Parsaie A.Prediction of side weir discharge coefficient by support vector machine technique. Water Science and Technology: Water Supply, 2016
17. Nguyen-Thanh N, Kiendl J, Nguyen-Xuan H, Wüchner R, Bletzinger K U, Bazilevs Y, Rabczuk T. Rotation free isogeometric thin shell analysis using PHT-splines. Computer Methods in Applied Mechanics and Engineering, 2011, 200(47–48): 3410–3424
18. Parsaie A. Analyzing the distribution of momentum and energy coefficients in compound open channel. Modeling Earth Systems and Environment, 2016, 2(1): 1–5
19. Rabczuk T, Areias P M A, Belytschko T. A meshfree thin shell method for non-linear dynamic fracture. International Journal for Numerical Methods in Engineering, 2007, 72(5): 524–548
20. Israelsen O W, Hansen V E. Irrigation Principles and Practices, Wiley, 1962
21. Negm A, El-Saiad A, Alhamid A, Husain D. Characteristics of simultaneous flow over weir and below inverted V-Notches Civil Engineering Research Magazine (CERM). Civil Engineering Department, Faculty of Engineering, Al-Azhar University, Cairo, Egypt, 1994, 16(9): 786–799
22. Negm A, El-Saiad A, Saleh O. Characteristics of combined flow over weirs and below submerged gates. In: Proceedings of the Al-Mansoura Eng. 2nd Int. Conf. (MEIC'97). 1997, 1–3
23. Ferro V. Simultaneous flow over and under a gate. Journal of Irrigation and Drainage Engineering, 2000, 126(3): 190–193
24. Negm A A M, Al-Brahim A M, Alhamid A A. Combined-free flow over weirs and below gates. Journal of Hydraulic Research, 2002, 40 (3): 359–365
25. Bagheri S, Heidarpour M. Overflow characteristics of circular-crested weirs. Journal of Hydraulic Research, 2010, 48(4): 515–520
26. Chanson H, Montes J S. Overflow characteristics of circular weirs: effects of inflow conditions. Journal of Irrigation and Drainage Engineering, 1998, 124(3): 152–162
27. Schmocker L, Halldórsdóttir B R, Hager W H. Effect of weir face angles on circular-crested weir flow. Journal of Hydraulic Engineering, 2011, 137(6): 637–643
28. Haghiabi A H. Hydraulic characteristics of circular crested weir based on Dressler theory. Biosystems Engineering, 2012, 112(4): 328–334
29. Kabiri-Samani A, Bagheri S. Discharge coefficient of circular-crested weirs based on a combination of flow around a cylinder and circulation. Journal of Irrigation and Drainage Engineering, 2014, 140(5): 04014010
30. Mohammadzadeh-Habili J, Heidarpour M, Afzalimehr H. Hydraulic characteristics of a new weir entitled of quarter-circular crested weir. Flow Measurement and Instrumentation, 2013, 33(0): 168–178
31. Severi A, Masoudian M, Kordi E, Roettcher K. Discharge coefficient of combined-free over-under flow on a cylindrical weir-gate. ISH Journal of Hydraulic Engineering, 2015, 21(1): 42–52
32. Azamathulla H, Ghani A. Genetic programming for predicting longitudinal dispersion coefficients in streams. Water Resources Management, 2011, 25(6): 1537–1544
33. Cai Y, Zhu H, Zhuang X. A continuous/discontinuous deformation analysis (CDDA) method based on deformable blocks for fracture modeling. Frontiers of Structural and Civil Engineering, 2013, 7(4): 369–378
34. Najafzadeh M, Azamathulla H M. Neuro-fuzzy GMDH to predict the scour pile groups due to waves. Journal of Computing in Civil Engineering, 2015, 29(5): 04014068
35. Najafzadeh M, Etemad-Shahidi A, Lim S Y. Scour prediction in long contractions using ANFIS and SVM. Ocean Engineering, 2016, 111: 128–135
36. Najafzadeh M, Sattar A A. Neuro-fuzzy GMDH approach to predict longitudinal dispersion in water networks. Water Resources Management, 2015, 29(7): 2205–2219
37. Najafzadeh M, Tafarojnoruz A. Evaluation of neuro-fuzzy GMDH-based particle swarm optimization to predict longitudinal dispersion coefficient in rivers. Environmental Earth Sciences, 2016, 75(2): 1–12
38. Parsaie A, Haghiabi A. Predicting the side weir discharge coefficient using the optimized neural network by genetic algorithm. Scientific Journal of Pure and Applied Sciences, 2014, 3(3): 103–112
39. Parsaie A, Yonesi H A, Najafian S. Predictive modeling of discharge in compound open channel by support vector machine technique. Modeling Earth Systems and Environment, 2015, 1(1–2): 1–6
40. Zhuang X, Augarde C E, Mathisen K M. Fracture modeling using meshless methods and level sets in 3D: Framework and modeling. International Journal for Numerical Methods in Engineering, 2012, 92(11): 969–998
41. Zhuang X Y, Huang R Q, Zhu H H, Askes H, Mathisen K. A new and simple locking-free triangular thick plate element using independent shear degrees of freedom. Finite Elements in Analysis and Design, 2013, 75: 1–7
42. Juma I A, Hussein H H, Al-Sarraj M F. Analysis of hydraulic characteristics for hollow semi-circular weirs using artificial neural networks. Flow Measurement and Instrumentation, 2014, 38: 49–53
43. Vu-Bac N, Lahmer T, Keitel H, Zhao J, Zhuang X, Rabczuk T. Stochastic predictions of bulk properties of amorphous polyethylene based on molecular dynamics simulations. Mechanics of Materials, 2014, 68: 70–84
44. Vu-Bac N, Lahmer T, Zhang Y, Zhuang X, Rabczuk T. Stochastic predictions of interfacial characteristic of polymeric nanocomposites (PNCs). Composites. Part B, Engineering, 2014, 59: 80–95
45. Vu-Bac N, Rafiee R, Zhuang X, Lahmer T, Rabczuk T. Uncertainty quantification for multiscale modeling of polymer nanocomposites

with correlated parameters. Composites. Part B, Engineering, 2015, 68: 446–464

46. Vu-Bac N, Silani M, Lahmer T, Zhuang X, Rabczuk T. A unified framework for stochastic predictions of mechanical properties of polymeric nanocomposites. Computational Materials Science, 2015, 96(B): 520–535